

Article

# Impact of Polarization Reversal during Photoelectrocatalytic Treatment of WWTP Effluents

Maria Cristina Collivignarelli <sup>1,2</sup>, Marco Carnevale Miino <sup>1</sup>, Francesca Maria Caccamo <sup>1</sup>, Alessandro Abbà <sup>3,\*</sup>, Massimiliano Bestetti <sup>4</sup> and Silvia Franz <sup>4</sup>

<sup>1</sup> Department of Civil Engineering and Architecture, University of Pavia, Via Ferrata 3, 27100 Pavia, Italy

<sup>2</sup> Interdepartmental Centre for Water Research, University of Pavia, Via Ferrata 3, 27100 Pavia, Italy

<sup>3</sup> Department of Civil, Environmental, Architectural Engineering and Mathematics, University of Brescia, Via Branze 43, 25123 Brescia, Italy

<sup>4</sup> Department of Chemistry, Materials and Chemical Engineering “Giulio Natta”, Politecnico di Milano, Via Mancinelli 7, 20131 Milano, Italy

\* Correspondence: alessandro.abba@unibs.it

**Abstract:** Photoelectrocatalysis (PEC) has been already proposed as a polishing treatment for wastewater treatment plants (WWTPs) effluents. In this work, the impact of polarization reversal during PEC process has been studied and evaluated on the basis of the removal of organic substance and color, biodegradability of the matrix, and inactivation of the catalyst. Effluents were sampled from a full-scale WWTP and alternatively treated by electrochemical oxidation (EC), photolysis (PL), photocatalysis (PC), photoelectrocatalysis, and photoelectrocatalysis with reverse polarization (PECr). The efficiency and the kinetics of the process, in terms of removal of organic substance and color, were not affected by reverse polarization and very similar results were obtained by PEC and PECr. The biodegradability of the effluents strongly increased both by PECr (RSBR:  $0.84 \pm 0.07$ ), and by PEC and PL ( $0.89 \pm 0.11$ , and  $0.78 \pm 0.02$ , respectively). In the selected polarization reversal mode (100 s at  $-0.1$  V every 500 s at 4 V, cell voltage), a similar photocurrent loss after PEC and PECr was observed, suggesting no effect on the activity of the TiO<sub>2</sub> mesh. This study can serve as a base for future research on polarization reversal to optimize operation parameters and exploit the procedure to preventing fouling and inactivation of the catalyst.

**Keywords:** photoelectrocatalysis; reverse polarization; fouling; catalyst inactivation; titanium dioxide; WWTP; polishing treatments

**Citation:** Collivignarelli, M.C.; Carnevale Miino, M.; Caccamo, F.M.; Abbà, A.; Bestetti, M.; Franz, S. Impact of Polarization Reversal during Photoelectrocatalytic Treatment of WWTP Effluents. *Environments* **2023**, *10*, 38. <https://doi.org/10.3390/environments10030038>

Academic Editor(s): William A. Anderson, Mehrab Mehrvar, Jason Zhang

Received: 30 January 2023

Revised: 16 February 2023

Accepted: 22 February 2023

Published: 25 February 2023



**Copyright:** © 2023 by the authors. Licensee MDPI, Basel, Switzerland. This article is an open access article distributed under the terms and conditions of the Creative Commons Attribution (CC BY) license (<https://creativecommons.org/licenses/by/4.0/>).

## 1. Introduction

Due to the production of hydroxyl ( $\bullet$ OH) radical species, which are characterized by a high redox potential (2.80 V), advanced oxidation processes (AOPs) are widely used to remove recalcitrant pollutants from water [1,2]. Several techniques have been already proposed in literature to produce hydroxyl radical species, and, among these, the interest in photoelectrocatalysis (PEC) is growing, as demonstrated by Palmas et al. [3]. They evaluated the number of documents on this topic in last 20 years, finding that almost half have been published in last 4 years. Moreover, comparing the types of journals in which older documents and more recent ones have been published, they proved that PEC is no longer applied only on a small laboratory scale, but also at a larger pilot-scale [3]. However, experience of PEC for water treatment at the full scale is relatively limited with few applications [4].

In heterogeneous photocatalysis (PC) on suspended catalyst, under suitable irradiation, electrons in the valence band are excited to the conduction band, leaving holes which can directly oxidize the organic substances or take part in the production of  $\bullet$ OH [5,6]. The main disadvantages of this process are represented by: (i) the need of a

subsequent sedimentation phase to collect and separate the catalyst powders from water flux; (ii) the phenomenon of the electron-hole recombination, which usually hampers  $\bullet\text{OH}$  [7,8]; and (iii) possible reduction reactions occurring at the same time on the same powders. In PEC, the addition of an electrical bias minimizes spontaneous electron-hole recombination, promoting  $\bullet\text{OH}$  production. Moreover, to overcome the settling issue, the photoanode catalyst is immobilized as supported semiconductor. In this case, the active surface area is reduced with respect to dispersed powders preferentially used in PC, but this disadvantage is generally compensated by the higher production of  $\bullet\text{OH}$  due to minimized electron-hole recombination [9].

Several semiconductors can be used to produce the photoanodes used in PEC [10–13], among which,  $\text{TiO}_2$  is the most investigated because of its many advantages, such as: (i) low cost, (ii) high availability, (iii) strong catalytic activity, (iv) non-toxicity, and (v) high chemical and photochemical stability [14–18].

Liu et al. [19] deeply studied the use of  $\text{TiO}_2$  in PEC to quantitatively evaluate the electron and hole transfer dynamics at the catalyst/water interface. Contrary to previous studies, which were performed on the limited time scales, in this case, they analyzed a longer timescale to identify primary water oxidation and reduction reactions of photo-excited anatase  $\text{TiO}_2$  films. They proved that most electrons and holes generated by light absorption generally recombine very quickly (ns). Therefore,  $\text{TiO}_2$  can be used as photocatalyst for water treatment, but an external bias application of at least to +0.5 V vs. Ag/AgCl is required to limit the recombination [19].

In addition to the applied potential bias, the effectiveness of PEC is also influenced by (i) the eventual catalyst manipulation, e.g., by doping with elements to optimize the absorption of UV light, and therefore the activation; and (ii) the electrochemical reactor design, which should be structured in order to maximize the absorption of UV light by the catalyst and facilitate the mass transfer in aqueous electrolyte [20].

One of the main limitations of PEC is represented by photoanode inactivation due to fouling of the active surface [21]. In fact, pollutants in water and products of degradative reactions can deposit on the surface of the catalyst. Murgolo et al. presented the chemical cleaning in dilute HCl solution as a valid solution to limit catalyst fouling, despite, in some cases, a re-anodization process is required [22].

In other electrochemical processes, such as electrocoagulation, periodic polarization reversal has been tested to reduce fouling. For instance, Chow and Pham [23] reported that during electrocoagulation, the effect of polarization reversal on fouling depends on the electrode material (i.e., it is effective with Al electrodes, but not with Fe electrodes). However, to the authors knowledge, this issue is still under investigated and further research is needed to understand fouling mechanisms and minimize the phenomenon.

In previous works, PEC has been proposed as polishing treatment of WWTPs' effluents containing residual organic matter and chromophore substances [18,24], but the adoption of reverse polarization during photoelectrocatalytic treatment of polluted waters has never been investigated.

This work aims to test the influence of polarization reversal during photoelectrocatalytic treatment of a WWTP's effluent. The effectiveness of polarization reversal has been evaluated on the basis of polishing efficiency and catalyst photoelectrochemical activity. Organic substance degradation, color removal, and biodegradability have been studied and a comparison with conventional photoelectrocatalysis and photolysis has been made. Additionally, photocurrent loss after each treatment test has been measured to monitor the photoanode activity and evaluate the influence of polarization reversal on the inactivation of catalyst during treatment of WWTP's effluent.

## 2. Materials and Methods

### 2.1. Characterization of TiO<sub>2</sub> Catalyst

The TiO<sub>2</sub> photoanode was obtained by Plasma Electrolytic Oxidation (PEO) of a Grade 1 titanium mesh (Nanomaterials S.r.l.). PEO was carried out in a 1.5 M H<sub>2</sub>SO<sub>4</sub> aqueous solution (14.7 wt%) for 9 min, at a constant potential of 150 V (EA-PSI 8360-15 T, EA Elektro-Automatik GmbH & Co., Viersen, Germany). The initial temperature of electrolyte was −5 °C (HAAK D10 cryostat, ENCO S.r.l.) [25,26]. Prior to PEO, the Ti mesh was chemically etched in an aqueous solution containing 25% HF—15% HNO<sub>3</sub>—60% H<sub>2</sub>O for 20 s and thoroughly rinsed in water. After PEO, the TiO<sub>2</sub> mesh was rinsed in water and air-dried.

Based on Scanning Electron Microscopy (SEM, EVO 50, Zeiss, Oberkochen, Germany), the TiO<sub>2</sub> oxide layer was porous, with submicrometric pores interconnected in a sponge-like surface morphology. The surface porosity was about 10% (ImageJ open-source software, version 1.52s) [27]. The thickness was determined by Glow Discharge Optical Emission Spectrometry (GD-OES, GDA750 analyzer, Spectruma Analytik GmbH) operated at 700 V in argon atmosphere at 230 Pa, and was about 2.5 nm. The geometric area of the mesh was 419 cm<sup>2</sup> (Leica DFC290, Microcontrol N.T., Milano, Italy). The Electrochemical Surface Area (ECSA) was measured by cyclic voltammetry [28], where consecutive potential cycles in a range of about ±50 mV centered around the open circuit potential were recorded at five different scan rates. The total electrochemical surface area of the TiO<sub>2</sub> photoanode was about 2.157 m<sup>2</sup>, in good agreement with the corresponding values obtained by ECSA and Brunauer–Emmett–Teller (BET) analysis in previous works [26].

The crystallographic structure of TiO<sub>2</sub> films was assessed by X-ray diffraction (XRD) (Philips PW1830) in Bragg-Brentano geometry. As shown in previous works, the TiO<sub>2</sub> film consisted in a mixture of anatase and rutile allotropic phases, with a relative composition of 58% and 42%, respectively [27].

The photoelectrochemical characterization of the TiO<sub>2</sub> mesh was carried out by Linear Scan Polarization (LSP) in a 4 mM KCl aqueous solution (2549 Model, Amel S.r.l., Milano, Italy) at a scan rate of 10 mV s<sup>−1</sup> and cell voltage in the range from 0 to 6 V. LSP was recorded in dark and under UV-C irradiation using a 30 W medium-pressure mercury light. After an initial sharp increase, the photocurrent density of the TiO<sub>2</sub> photoanode reaches a plateau value of 1.04 mA/cm<sup>2</sup>.

### 2.2. Properties of WWTP Effluents

The effluents were sampled at the final discharge of a WWTP located in northern Italy (population equivalents—PE: 60,000). The plant treats both urban and industrial wastewater with a conventional scheme of water line (biological conventional active sludge (CAS) with both nitrification and denitrification activities). No polishing treatments are present. Industrial wastewater is also pre-treated in a chemical-physical unit, and in a thermophilic biological process. Details of the plant where the effluents have been collected can be found in previous works [29,30].

Samples of wastewater treatment plant effluent (WWTPE) have been characterized, and main properties are reported in Table 1. The pH was almost neutral with a moderate electrical conductivity. The UV absorbance at 254 nm was 0.4–0.5 (the entire UV-vis absorbance spectra is reported in Figure S1). The functioning of UV system used in this work is ensured by the low TSS concentration in the water (Table 1).

**Table 1.** Main properties of WWTPE. u.m.: unit of measure; COD: chemical oxygen demand; UV<sub>254</sub>: absorbance at 254 nm; ECon: electrical conductivity; TSS: total suspended solids; SOUR: specific oxygen uptake rate calculated according to [31]; VSS: volatile suspended solids.

Parameter [u.m.]	Value
COD [mg L <sup>-1</sup> ]	75–80
UV <sub>254</sub> [A.U.]	0.40–0.50
pH [–]	7.5–7.9
ECon [mS cm <sup>-1</sup> ]	2500–2900
TSS [mg L <sup>-1</sup> ]	15–25
SOUR [mg <sub>O2</sub> g <sub>VSS</sub> <sup>-1</sup> h <sup>-1</sup> ]	2–2.5
Color	Light yellow

### 2.3. Experimental Set-Up and Lab-Scale Reactor

Five different treatments have been tested and compared:

- Electrochemical oxidation (EC): TiO<sub>2</sub> + bias
- Photolysis (PL): UV
- Photocatalysis (PC): UV + TiO<sub>2</sub>
- Photoelectrocatalysis (PEC): UV + TiO<sub>2</sub> + bias
- Photoelectrocatalysis with polarization reversal (PECr): UV + TiO<sub>2</sub> + reverse bias.

In the present study, all tests except for PL were carried out using supported TiO<sub>2</sub> mesh to avoid subsequent sedimentation phase. Each treatment was repeated twice, and it was carried out for a reaction time equals to 2 h. After each test, the mesh was cleaned by immersion in a diluted HCl solution (0.9 M) for 30 min.

Tests have been carried out at room temperature (~20–25 °C) using a lab-scale equipment composed by: (i) an electrochemical reactor which operated in up-flow mode (1 L), (ii) a tank (2.4 L), and (iii) a pump (Iwaki Magnet Pump MD-30RZ-220 N with 80 kW of nominal power) for water recirculation. The scheme of the system is reported in Figure 1.

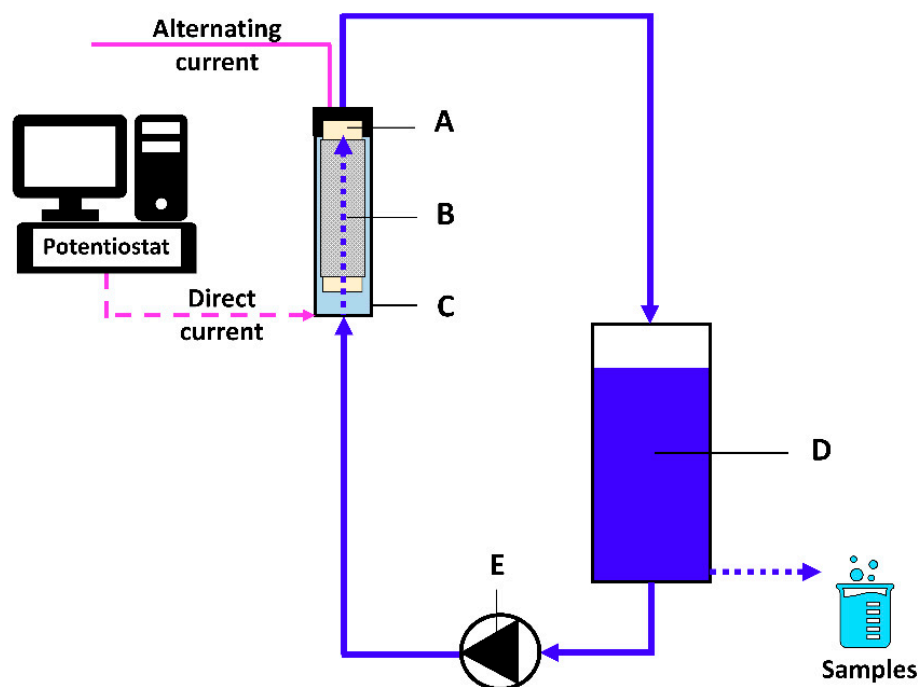


**Figure 1.** Scheme of the laboratory-scale reactor working in up-flow condition and semi-batch mode. A: lamp, B: TiO<sub>2</sub> mesh, C: electrochemical reactor, D: tank, and E: pump.

The system was operated in semi-batch mode and a turbulent flow inside the AISI 304 reactor was maintained. The reactor was equipped with a 30 W medium-pressure Hg vapor lamp having tubular shape (the emission spectra of the UV lamp is reported in

Figure S2). The anodized TiO<sub>2</sub> mesh was placed coaxially surrounding the UV lamp with a gap of few millimeters. A detailed description of the electrochemical reactor can be found in our previous works [7,18,22,24,32].

Samples (10 mL) have been taken every 10 min of reaction time from the tank. During the photoelectrocatalytic tests, the TiO<sub>2</sub> mesh and the reactor body were anodically and cathodically polarized, respectively, by a potentiostat/galvanostat (AMEL 2549) at constant cell voltage of 4 V. Before and after each treatment, this same instrument was used to evaluate the photoelectrochemical activity of the TiO<sub>2</sub> mesh. In PECr, every 500 s of reaction time, cell voltage was reversed applying −0.1 V for 100 s.

Additionally, to evaluate the aging of the TiO<sub>2</sub> catalyst along prolonged use in PEC processes, a set of five degradation tests was carried out, each test lasting 2 h of reaction time, without washing the TiO<sub>2</sub> mesh before or after each replicate. The efficiency of each test was evaluated on the basis of absorbance at 254 nm (UV<sub>254</sub>).

## 2.4. Evaluation of the Treatments Effectiveness

### 2.4.1. Pollutants Removal

To understand and compare the effectiveness of treatments, organic substance and color were monitored. The residual organic matter was evaluated based on absorbance at 254 nm (UV<sub>254</sub>), while the residual color (Color<sub>i</sub> Color<sub>0</sub><sup>−1</sup>) was determined by integrating the UV-Vis absorbance spectrum in the range from 356 nm to 700 nm (IA) [24,33] according to the following Equation (1):

$$\text{Color}_i/\text{Color}_0 (-) = \text{IA}_i/\text{IA}_0, \quad (1)$$

where IA<sub>i</sub> is the integral of the absorbance spectrum at t = i, and IA<sub>0</sub> is the integral of the absorbance spectrum at t = 0.

Absorbance spectra of treated and untreated WWTPe were determined by means of UV-Vis spectrophotometry (HP 8453, Agilent Technologies Deutschland GmbH, Waldbronn, Germany).

For a straightforward comparison and evaluation of the tests, the Langmuir–Hinshelwood kinetic model (LHM) approximated at the first order was applied both for organic substance and color removal (Equations (2) and (3)).

$$\ln(C_i/C_0) = -k \times t, \quad (2)$$

$$\text{HLT} = \ln(2)/k, \quad (3)$$

where C<sub>0</sub> and C<sub>i</sub> represent the pollutants concentration (organic substance or color) in the initial and i-th samples, respectively. The half-life time (HLT) of the pollutants has been calculated based on the pseudo-first order kinetic constant of the reaction (k).

### 2.4.2. Biodegradability of the Water

According to our previous work [34], an index correlating the SOUR by biota and the removed organic matter was used to evaluate the impact of different treatments on the biodegradability of the WWTPe. Relative Specific Biodegradation Rate (RSBR) was calculated following Equation (4):

$$\text{RSBR} (-) = [(\text{SOUR}_i - \text{SOUR}_0)/(\text{SOUR}_i + \text{SOUR}_0)] + [(\text{COD}_0 - \text{COD}_i)/(\text{COD}_0 + \text{COD}_i)] \quad (4)$$

where SOUR<sub>0</sub> and COD<sub>0</sub> are the value of specific oxygen uptake rate and chemical oxygen demand in the untreated WWTPe, while SOUR<sub>i</sub> and COD<sub>i</sub> represent the values the i-th sample. RSBR can vary from −1 (low biodegradability of the treated sample compared to untreated one) to 2 (high biodegradability of the treated sample compared to initial WWTPe). If the biodegradability is not affected by the treatment, RSBR is close to 0.

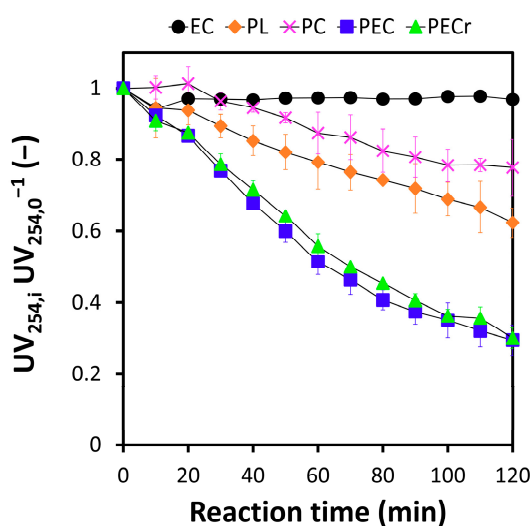
According to the procedure described by Collivignarelli et al. [35], oxygen uptake rate (OUR) tests have been carried out using a mesophilic biomass sampled in the CAS system of the same WWTP and SOUR has been expressed as  $[\text{mgO}_2 \text{ gVSS}^{-1} \text{ h}^{-1}]$ . COD was measured following the ISPRA 5135 method [36].

### 3. Results and Discussion

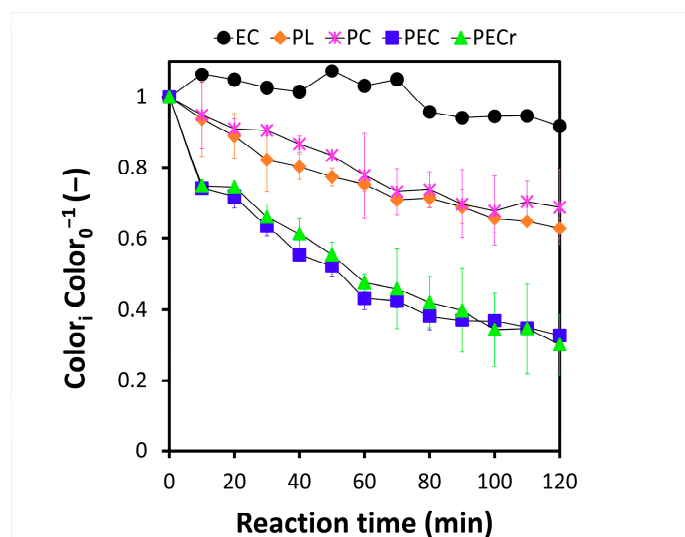
#### 3.1. Pollutants Degradation

Figure 2a,b show the performance in removal of organic substance and color by PECr, EC, PL, PC, and PEC tests. In Figure S3, the samples after 2 h of treatment are presented. PECr allowed to obtain very similar results as by PEC, being the removal of organic substance and color after 2 h of reaction time  $\approx 70\%$  and  $68\%$ , respectively. Therefore, the polarization reversal (100 s every 500 s of direct bias) did not significantly affect the oxidation kinetics.

According to previous works [7,37,38], EC showed a negligible degradation effect due to the absence of UV source able to activate the catalyst. This trend was observed both for  $\text{UV}_{254}$  and color for which, after 2 h of reaction time, only 3.2% and 8.3% were removed, respectively.



(a)



(b)

**Figure 2.** (a) Residual  $\text{UV}_{254}$  ( $\text{UV}_{254,i} / \text{UV}_{254,0}^{-1}$ ), and (b) residual color ( $\text{Color}_i / \text{Color}_0^{-1}$ ) relative to the corresponding parameters at  $t = 0$  during EC, PL, PC, PEC, and PECr tests. Confidence intervals have been calculated based on two replicates.

As for the PC tests, previous studies demonstrated that the removal performance of organics by conventional PC using suspended  $\text{TiO}_2$  powders is comparable with PEC tests, despite the catalytic surface area in PEC was one order of magnitude lower than in PC [22]. The PEC performance was obviously attributed to the compensation effect provided by the applied bias, resulting in a minimization of electron-hole recombination phenomena [9,26,39].

In the present study, the PC tests were carried out using supported  $\text{TiO}_2$  mesh: this set-up, chosen to avoid subsequent sedimentation phase, significantly reduced the active surface for  $\text{OH}^\bullet$  production without the compensation effect given by bias application. This reasonably explains the increase of HLT and reduction of  $k$  values compared to PEC (Figure 3).

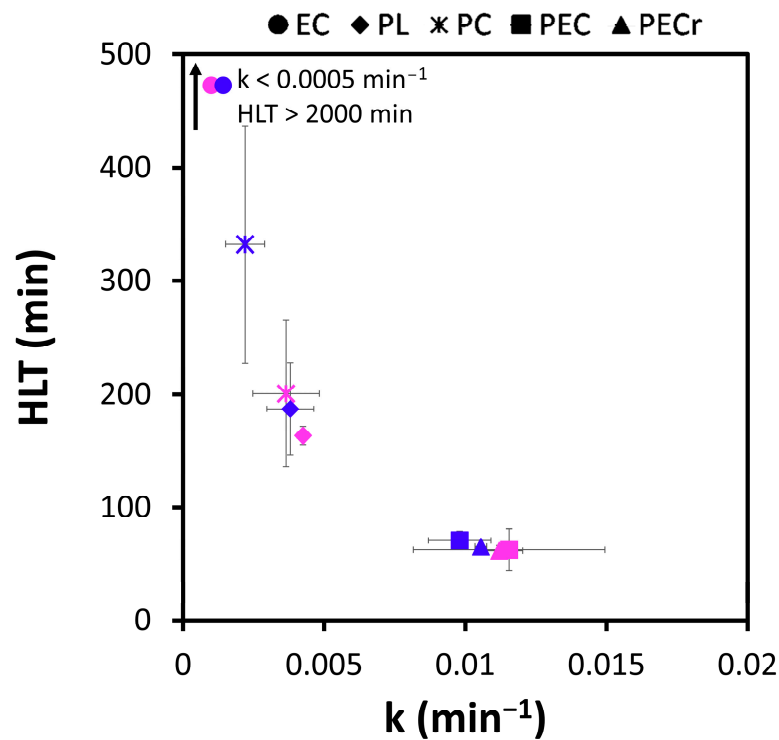


**Figure 3.** Pseudo first-order kinetic constants  $k$  using the Langmuir–Hinshelwood model, and corresponding HLT of EC, PL, PC, PEC, and PECr tests for  $UV_{254}$  (blue data), and color removal (pink data). Confidence intervals have been calculated based on two replicates.

The degradation kinetics of PL tests was faster than PC. After 2 h of reaction time, PL removed almost 38% of organic substance and color, which is higher than PC ( $\approx 22\%$  and  $31\%$  for  $UV_{254}$  and color, respectively). Correspondingly, the kinetic constants showed lower values in PC compared to PL ( $0.0022 \text{ min}^{-1}$  vs.  $0.0038 \text{ min}^{-1}$  for  $UV_{254}$ , and  $0.0037 \text{ min}^{-1}$  vs.  $0.0043 \text{ min}^{-1}$  for color). This can be attributed to the shielding effect of the  $TiO_2$  mesh on the UV lamp. Our previous studies demonstrated that operating with this reactor configuration, the catalytic mesh shields more than 50% of UV dosage reaching the water sample [22,24].

Focusing on the relation between the photocurrent of the  $TiO_2$  mesh, and  $UV_{254}$  and color removal, two different clusters can be identified: EC-PC (*cl.a*), and PEC-PECr (*cl.b*) (Figure 4).

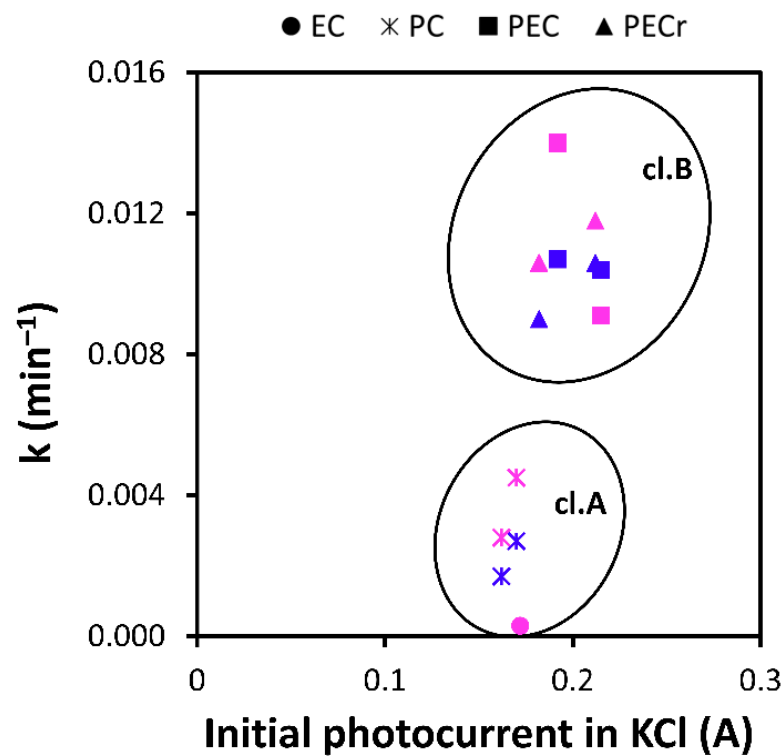


**Figure 4.** Initial photocurrent and first-order kinetic constants using the Langmuir–Hinshelwood model of EC, PC, PEC, and PECr for UV<sub>254</sub> (blue data), and color removal (pink data). cl: cluster.

Despite the average initial photocurrent being about 0.18–0.20 A for both clusters, in *cl.a*, the values of the pseudo first-order kinetic constants for organic substance removal were significantly lower than those of *cl.b* (representing PEC–PECr). This can be explained considering that photoelectrochemical measurements accounted for the synergistic effect of irradiation and electrochemical polarization, which developed in PEC and PECr, but not in PC or EC tests. Therefore, it is reasonable to expect that this parameter does not discriminate between the different tests. Any relation between the photocurrent of the mesh and the kinetic constant was observed within the *cl.b*, probably suggesting that the kinetics of photoelectrocatalytic processes depend only to some extent on the photoelectrochemical response in model electrolytes, and other surface phenomena concurring to determine the value of the kinetic constants.

### 3.2. Effects on Biodegradability

The effect on biodegradability of the effluents was evaluated studying the RSBR as a function of reaction time. PECr gave very similar results to PEC and PL, significantly increasing the biodegradability (RSBR > 0) of the effluent compared with the untreated sample (RSBR = 0) (Figure 5). This means that these processes were able not only to remove organic matter but also to change the chemistry of the pollutants, making them more suitable for the mesophilic biota.

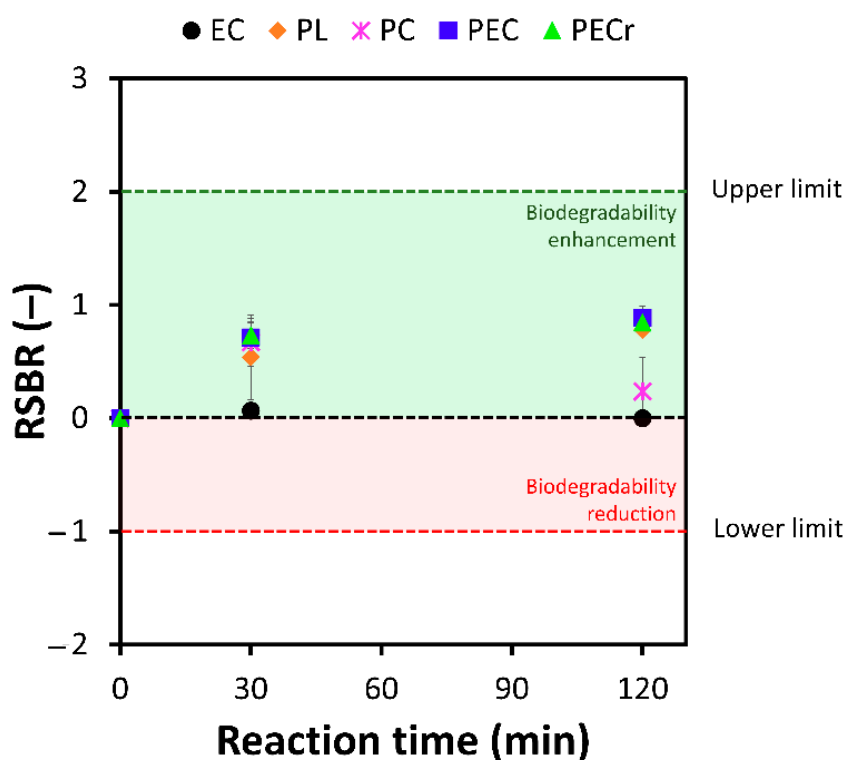


**Figure 5.** RSBR of EC, PC, PEC, and PECr.

On the contrary, EC was not able to affect the biodegradability of the matrix, confirming the results obtained in terms of organic substance removal (Section 3.1). PC improved the biodegradability, although not as much as PL, PEC, and PECr. This result, as previously discussed for  $UV_{254}$  and color, can be attributed to the shielding of more than 50% of UV dosage when the  $TiO_2$  mesh was placed around the UV lamp [22,24]. While electrical polarization in PECr and PEC allowed the overcoming this phenomenon by minimizing electron-hole recombination, in PC a reduction in organic substance degradation with respect to PL was observed.

The reaction time significantly affected the RSBR especially in the initial stage of the tests, reaching values of  $0.54 \pm 0.37$ ,  $0.71 \pm 0.13$ , and  $0.73 \pm 0.12$  for PL, PEC, and PECr, respectively. The extension of the processes up to 120 min induced a less pronounced increase in the RSBR parameter, which was  $0.78 \pm 0.02$ ,  $0.89 \pm 0.11$ , and  $0.84 \pm 0.07$  for PL, PEC, and PECr, respectively. This is reasonably explained considering that two classes of chemical organic bonds can be distinguished: the weaker ones are oxidized relatively quickly, i.e., within the first 30 min of the processes, while the stronger ones require a much longer process time to be oxidized and allow a further increase in the biodegradability of the sample.

### 3.3. Mesh Inactivation and Influence of Reverse Polarization

For a tentative assessment of photoelectrode inactivation rate, PEC tests were replicated five times, for a total usage of 30 h of process time. No washing of the  $TiO_2$  mesh was carried out between subsequent tests. Based on  $UV_{254}$  data as a function of reaction time (Figure 6), a slight reduction in degradation efficiency can be inferred, the pseudo-kinetic constants of the PEC replicates decreasing from  $0.01336 \text{ min}^{-1}$  (PEC 1) to  $0.01247 \text{ min}^{-1}$  (PEC 3), and finally to  $0.01183 \text{ min}^{-1}$  (PEC 5). On the contrary, the HLT increased from 51.9 min in PEC1 to 58.6 min after five time of consecutive use of the mesh.

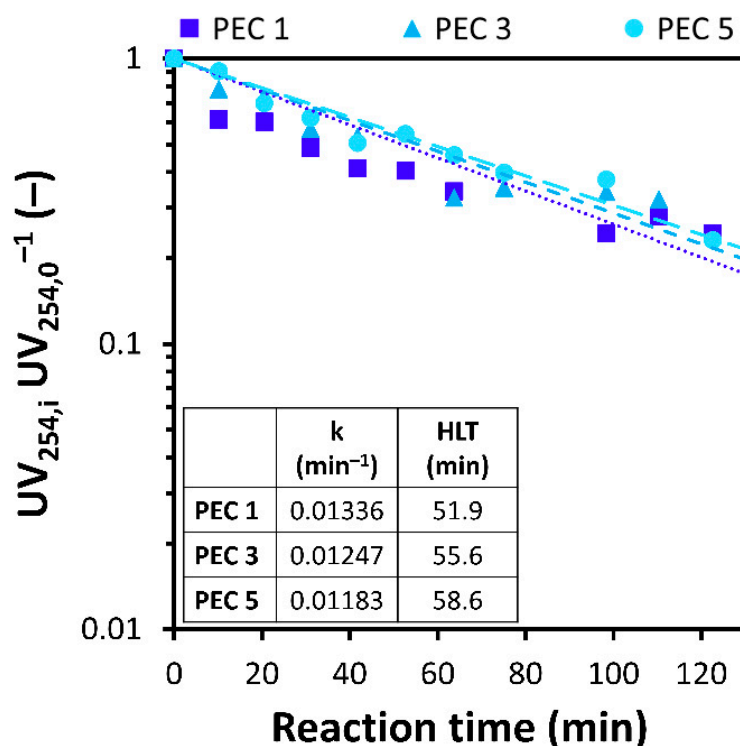


**Figure 6.** Aging effect of the nanostructured TiO<sub>2</sub> meshes under repeated use in PEC process. PEC 1, PEC 3, and PEC 5 represent the UV<sub>254</sub> removal after one, three, and five-time use.

The average inactivation rate, calculated on the basis of the  $k$  values, is 11.5% after five cycles of treatments (2 h of reaction time, and 6 h of processing time per each cycle). The TiO<sub>2</sub> mesh inactivation can be attributed to surface fouling, probably induced by by-products adsorption, precipitation, or filming.

In other electrochemical processes, polarization reversal was already proposed to reduce fouling problems, as in the electrocoagulation. The accumulation of an insulating surface layer increases the resistance of the electron-transfer processes at the electrode-electrolyte interfaces and, therefore, the effectiveness of the process [40,41]. Indeed, in the cathodic part the fouling by-products can be removed either by electrochemical reduction, or by mechanical detachment due to hydrogen evolution. The polarization reversal in the electrocoagulation processes did not gave positive results in all cases and periodic mechanical removal was preferred [40,41].

Moreover, the acid cleaning of the anode has been proposed as a possible solution to mitigate the fouling of catalyst in PEC processes [22]. In this work, polarization reversal is investigated as a possible strategy to reduce photocatalyst inactivation due to layering of the electrode surface.

Therefore, this application can potentially help not only to remove fouling layers already present in the catalyst, but also to prevent their formation. However, the number of studies focused on the application of this technique on PEC during the treatment of water is still limited and further research is needed.

Our study ruled out the possibility that periodically reverting the polarization could negatively affect the performance of the photoelectrochemical process (Sections 3.1 and 3.2). However, this work aims to evaluate if the polarization reversal can be applied as an anti-fouling technique in PEC.

The photocurrent loss after one cycle of treatments of EC, PC, PEC, and PECr have been compared and similar values were observed (Figure 7). This further confirms that the selected polarization curve (100 s at  $-0.1$  V, and 500 s at 4 V, respectively) did not affect

catalyst inactivation. However, it is the authors opinion that this aspect should be further investigated.

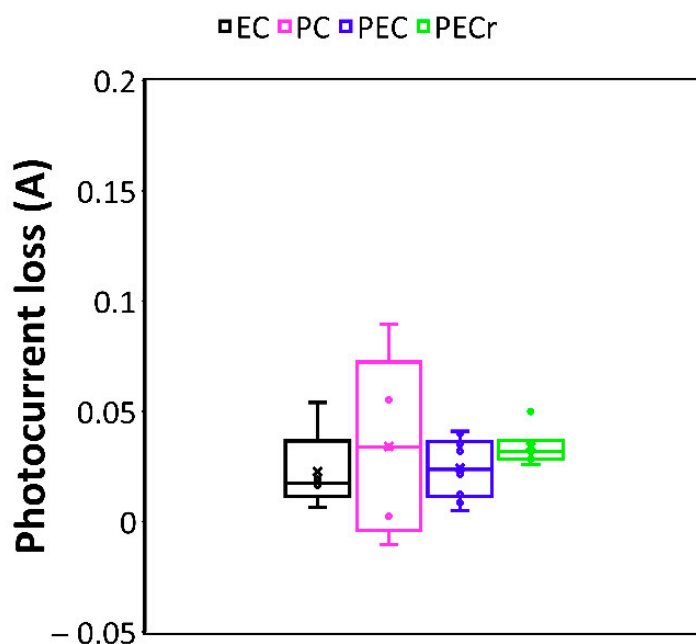


**Figure 7.** Photocurrent loss of the TiO<sub>2</sub> mesh after one test (reaction time: 2 h). Confidence intervals have been calculated based on five replicates.

In future studies the aging effect of the nanostructured TiO<sub>2</sub> meshes in PECr process should be evaluated in case of prolonged use. Moreover, the value of the cathodic voltage, and the duration and frequency of the cathodic stage during polarization reversal should be optimized to evaluate how they affect the fouling removal, and the catalyst reactivation in photoelectrochemical systems.

#### 4. Conclusions

The impact of polarization reversal during the photoelectrocatalytic treatment of WWTPs effluents has been investigated. The selected polarization reversal mode, consisting of 100 s at  $-0.1$  V, every 500 s at 4 V, did not affect the efficiency of the process in terms of removal of organic substance and color with respect to PEC. Indeed, after 2 h of reaction time the removal of organic substance and color was  $\approx 70\%$  and  $68\%$  for PECr and PEC, respectively. The pollutants removal rate followed the order:  $PEC \approx PECr > PL > PC > EC$ . PECr, PEC, and PL were able to significantly enhance the biodegradability of the effluents (RSBR:  $0.84 \pm 0.07$ ,  $0.89 \pm 0.11$ , and  $0.78 \pm 0.02$ , for PECr, PEC, and PL, respectively), while PC and EC did not affect it. Based on the absorbance at 254 nm, the inactivation of the mesh was  $-11.5\%$  after 5 PEC replicates (30 h overall processing time). The photocurrent loss after a single test was very similar in EC, PC, and PEC, regardless the polarization reversal, suggesting that this parameter cannot discriminate between different configurations and that it accounts only to a certain extent for the photoelectrocatalytic activity of the mesh. Based on these results, the authors suggest: (i) to further investigate the aging effect of the nanostructured TiO<sub>2</sub> meshes in PECr process in case of prolonged use, and to (ii) optimize the values of parameters (e.g., cathodic voltage, and the duration and frequency of the cathodic stage) during polarization reversal to evaluate how they affect the fouling removal, and catalyst reactivation in photoelectrochemical systems.

**Supplementary Materials:** The following supporting information can be downloaded at: <https://www.mdpi.com/article/10.3390/environments10030038/s1>, Figure S1. UV-Vis absorbance spectra of the untreated WWTP; Figure S2. Emission spectra of medium-pressure Hg vapor lamp used in the study; Figure S3. Samples of untreated water and after 2 h of EC, PL, PC, PEC and PECr.

**Author Contributions:** Conceptualization, M.C.C., M.C.M., M.B., and S.F.; methodology, M.C.C. and S.F.; validation, M.C.C. and S.F.; formal analysis, M.C.M. and F.M.C.; investigation, M.C.M. and F.M.C.; resources, M.C.C., M.B., and S.F.; data curation, M.C.M. and F.M.C.; writing—original draft preparation, M.C.M. and S.F.; writing—review and editing, M.C.C., M.C.M., A.A., and S.F.; visualization, M.C.M. and A.A.; supervision, M.C.C. and S.F.; funding acquisition, M.C.C., M.B., and S.F. All authors have read and agreed to the published version of the manuscript.

**Funding:** This research was partially funded by ASMia S.r.l. (ASMortara S.p.A. Group).

**Institutional Review Board Statement:** Not applicable.

**Informed Consent Statement:** Not applicable.

**Data Availability Statement:** All data generated or analyzed during this study are included in this published article.

**Acknowledgments:** The authors acknowledge ASMia S.r.l. (ASMortara S.p.A. Group), Daniele Aieta, and Alessandro Pietro Tucci (Politecnico di Milano) for giving the technical support to the experimental research.

**Conflicts of Interest:** The authors declare no conflict of interest.

## Nomenclature

AOPs: advanced oxidation processes; BET: Brunauer–Emmett–Teller; CAS: conventional active sludge; cl: cluster; COD: chemical oxygen demand; EC: electrochemical oxidation; ECon: electrical conductivity; ECSA: electrochemical surface area; GD-OES: glow discharge optical emission spectrometry; HLT: half-life time; LHM: Langmuir–Hinshelwood kinetic model; LSP: linear scan polarization; OUR: oxygen uptake rate; PC: photocatalysis; PEC: photoelectrocatalysis; PECr: photoelectrocatalysis with reverse polarization; PEO: plasma electrolytic oxidation; PL: photolysis; RSBR: relative specific biodegradation rate; SEM: scanning electron microscopy; SOUR: specific oxygen uptake rate; TSS: total suspended solids; UV<sub>254</sub>: absorbance at 254 nm; VSS: volatile suspended solids; WWTP: wastewater treatment plant; WWTPe: wastewater treatment plant effluent; XRD: X-ray diffraction.

## References

1. Oturan, M.A.; Aaron, J.-J. Advanced Oxidation Processes in Water/Wastewater Treatment: Principles and Applications. A Review. *Crit. Rev. Environ. Sci. Technol.* **2014**, *44*, 2577–2641. <https://doi.org/10.1080/10643389.2013.829765>.
2. Oller, I.; Malato, S.; Sánchez-Pérez, J.A. Combination of Advanced Oxidation Processes and Biological Treatments for Wastewater Decontamination—A Review. *Sci. Total Environ.* **2011**, *409*, 4141–4166.
3. Palmas, S.; Mais, L.; Mascia, M.; Vacca, A. Trend in Using TiO<sub>2</sub> Nanotubes as Photoelectrodes in PEC Processes for Wastewater Treatment. *Curr. Opin. Electrochem.* **2021**, *28*, 100699. <https://doi.org/10.1016/j.coelec.2021.100699>.
4. Brillas, E.; Garcia-Segura, S. Benchmarking Recent Advances and Innovative Technology Approaches of Fenton, Photo-Fenton, Electro-Fenton, and Related Processes: A Review on the Relevance of Phenol as Model Molecule. *Sep. Purif. Technol.* **2020**, *237*, 116337. <https://doi.org/10.1016/j.seppur.2019.116337>.
5. Ameta, R.; Solanki, M.S.; Benjamin, S.; Ameta, S.C. Photocatalysis. In *Advanced Oxidation Processes for Waste Water Treatment*; Elsevier: Amsterdam, The Netherlands, 2018; pp. 135–175.
6. Mills, A.; O'Rourke, C.; Moore, K. Powder Semiconductor Photocatalysis in Aqueous Solution: An Overview of Kinetics-Based Reaction Mechanisms. *J. Photochem. Photobiol. A Chem.* **2015**, *310*, 66–105. <https://doi.org/10.1016/j.jphotochem.2015.04.011>.
7. Franz, S.; Perego, D.; Marchese, O.; Bestetti, M. Photoelectrochemical Advanced Oxidation Processes on Nanostructured TiO<sub>2</sub> Catalysts: Decolorization of a Textile Azo-Dye. *J. Water Chem. Technol.* **2015**, *37*, 108–115. <https://doi.org/10.3103/S1063455X15030029>.
8. Yusuf, T.L.; Orimolade, B.O.; Masekela, D.; Mamba, B.; Mabuba, N. The Application of Photoelectrocatalysis in the Degradation of Rhodamine B in Aqueous Solutions: A Review. *RSC Adv.* **2022**, *12*, 26176–26191. <https://doi.org/10.1039/D2RA04236C>.
9. Noorjahan, M.; Pratap Reddy, M.; Durga Kumari, V.; Lavédrine, B.; Boule, P.; Subrahmanyam, M. Photocatalytic Degradation of H-Acid over a Novel TiO<sub>2</sub> Thin Film Fixed Bed Reactor and in Aqueous Suspensions. *J. Photochem. Photobiol. A Chem.* **2003**, *156*, 179–187. [https://doi.org/10.1016/S1010-6030\(02\)00408-2](https://doi.org/10.1016/S1010-6030(02)00408-2).

10. Baccaro, A.; Gutz, I. Photoelectrocatalysis in Semiconductors: From Basic Principles to Nanoscale Conformation (in Portuguese). *Quim. Nova* **2018**, *41*, 326–339. <https://doi.org/10.21577/0100-4042.20170174>.
11. Chen, W.; Liu, S.; Fu, Y.; Yan, H.; Qin, L.; Lai, C.; Zhang, C.; Ye, H.; Chen, W.; Qin, F.; et al. Recent Advances in Photoelectrocatalysis for Environmental Applications: Sensing, Pollutants Removal and Microbial Inactivation. *Coord. Chem. Rev.* **2022**, *454*, 214341. <https://doi.org/10.1016/j.ccr.2021.214341>.
12. Bessegato, G.G.; Guaraldo, T.T.; de Brito, J.F.; Brugnera, M.F.; Zanoni, M.V.B. Achievements and Trends in Photoelectrocatalysis: From Environmental to Energy Applications. *Electrocatalysis* **2015**, *6*, 415–441. <https://doi.org/10.1007/s12678-015-0259-9>.
13. Olea, M.A.U.; Bueno, J.d.J.P.; Pérez, A.X.M. Nanometric and Surface Properties of Semiconductors Correlated to Photocatalysis and Photoelectrocatalysis Applied to Organic Pollutants—A Review. *J. Environ. Chem. Eng.* **2021**, *9*, 106480. <https://doi.org/10.1016/j.jece.2021.106480>.
14. Komtchou, S.; Dirany, A.; Drogui, P.; Delegan, N.; El Khakani, M.A.; Robert, D.; Lafrance, P. Degradation of Atrazine in Aqueous Solution with Electrophotocatalytic Process Using TiO<sub>2-x</sub> Photoanode. *Chemosphere* **2016**, *157*, 79–88. <https://doi.org/10.1016/j.chemosphere.2016.05.022>.
15. Malato, S. Removal of Emerging Contaminants in Waste-Water Treatment: Removal by Photo-Catalytic Processes. In *Emerging Contaminants from Industrial and Municipal Waste. The Handbook of Environmental Chemistry*; Springer: Berlin/Heidelberg, Germany, 2008; pp. 177–197.
16. Luster, E.; Avisar, D.; Horovitz, I.; Lozzi, L.; Baker, M.A.; Grilli, R.; Mamane, H. N-Doped TiO<sub>2</sub>-Coated Ceramic Membrane for Carbamazepine Degradation in Different Water Qualities. *Nanomaterials* **2017**, *7*, 206. <https://doi.org/10.3390/nano7080206>.
17. Ghosh, M.; Lohrasbi, M.; Chuang, S.S.C.; Jana, S.C. Mesoporous Titanium Dioxide Nanofibers with a Significantly Enhanced Photocatalytic Activity. *ChemCatChem* **2016**, *8*, 2525–2535. <https://doi.org/10.1002/cctc.201600387>.
18. Collivignarelli, M.C.; Abbà, A.; Carnevale Miino, M.; Bertanza, G.; Sorlini, S.; Damiani, S.; Arab, H.; Bestetti, M.; Franz, S. Photoelectrocatalysis on TiO<sub>2</sub> Meshes: Different Applications in the Integrated Urban Water Management. *Environ. Sci. Pollut. Res.* **2021**, *28*, 59452–59461. <https://doi.org/10.1007/s11356-021-12606-5>.
19. Liu, H.; Liu, M.; Nakamura, R.; Tachibana, Y. Primary Photocatalytic Water Reduction and Oxidation at an Anatase TiO<sub>2</sub> and Pt-TiO<sub>2</sub> Nanocrystalline Electrode Revealed by Quantitative Transient Absorption Studies. *Appl. Catal. B* **2021**, *296*, 120226. <https://doi.org/10.1016/j.apcatb.2021.120226>.
20. Wang, Y.; Zu, M.; Zhou, X.; Lin, H.; Peng, F.; Zhang, S. Designing Efficient TiO<sub>2</sub>-Based Photoelectrocatalysis Systems for Chemical Engineering and Sensing. *Chem. Eng. J.* **2020**, *381*, 122605. <https://doi.org/10.1016/j.cej.2019.122605>.
21. Egerton, T.A.; Christensen, P.A.; Kosa, S.A.M.; Onoka, B.; Harper, J.C.; Tinlin, J.R. Photoelectrocatalysis by Titanium Dioxide for Water Treatment. *Int. J. Environ. Pollut.* **2006**, *27*, 2. <https://doi.org/10.1504/IJEP.2006.010450>.
22. Murgolo, S.; Franz, S.; Arab, H.; Bestetti, M.; Falletta, E.; Mascolo, G. Degradation of Emerging Organic Pollutants in Wastewater Effluents by Electrochemical Photocatalysis on Nanostructured TiO<sub>2</sub> Meshes. *Water Res.* **2019**, *164*, 114920. <https://doi.org/10.1016/j.watres.2019.114920>.
23. Chow, H.; Pham, A.L.-T. Mitigating Electrode Fouling in Electrocoagulation by Means of Polarity Reversal: The Effects of Electrode Type, Current Density, and Polarity Reversal Frequency. *Water Res.* **2021**, *197*, 117074. <https://doi.org/10.1016/j.watres.2021.117074>.
24. Collivignarelli, M.C.; Carnevale Miino, M.; Arab, H.; Bestetti, M.; Franz, S. Efficiency and Energy Demand in Polishing Treatment of Wastewater Treatment Plants Effluents: Photoelectrocatalysis vs. Photocatalysis and Photolysis. *Water* **2021**, *13*, 821. <https://doi.org/10.3390/w13060821>.
25. Franz, S.; Perego, D.; Marchese, O.; Lucotti, A.; Bestetti, M. Photoactive TiO<sub>2</sub> Coatings Obtained by Plasma Electrolytic Oxidation in Refrigerated Electrolytes. *Appl. Surf. Sci.* **2016**, *385*, 498–505. <https://doi.org/10.1016/j.apsusc.2016.05.032>.
26. Franz, S.; Arab, H.; Chiarello, G.L.; Bestetti, M.; Selli, E. Single-Step Preparation of Large Area TiO<sub>2</sub> Photoelectrodes for Water Splitting. *Adv. Energy Mater.* **2020**, *10*, 2000652. <https://doi.org/10.1002/aenm.202000652>.
27. Franz, S.; Arab, H.; Lucotti, A.; Castiglioni, C.; Vincenzo, A.; Morini, F.; Bestetti, M. Exploiting Direct Current Plasma Electrolytic Oxidation to Boost Photoelectrocatalysis. *Catalysts* **2020**, *10*, 325. <https://doi.org/10.3390/catal10030325>.
28. Trasatti, S.; Petrii, O.A. Real Surface Area Measurements in Electrochemistry. *Pure Appl. Chem.* **1991**, *63*, 711–734. <https://doi.org/10.1351/pac199163050711>.
29. Collivignarelli, M.C.; Abbà, A.; Bertanza, G.; Damiani, S.; Raboni, M. Resilience of a Combined Chemical-Physical and Biological Wastewater Treatment Facility. *J. Environ. Eng.* **2019**, *145*, 05019002. [https://doi.org/10.1061/\(ASCE\)EE.1943-7870.0001543](https://doi.org/10.1061/(ASCE)EE.1943-7870.0001543).
30. Collivignarelli, M.C.; Todeschini, S.; Abbà, A.; Ricciardi, P.; Carnevale Miino, M.; Torretta, V.; Rada, E.C.; Conti, F.; Cillari, G.; Calatroni, S.; et al. The Performance Evaluation of Wastewater Service: A Protocol Based on Performance Indicators Applied to Sewer Systems and Wastewater Treatment Plants. *Environ. Technol.* **2022**, *43*, 3426–3443. <https://doi.org/10.1080/09593330.2021.1922509>.
31. Water Quality—Test for Inhibition of Oxygen Consumption by Activated Sludge for Carbonaceous and Ammonium Oxidation; ISO 8192:2007; International Organization for Standardization (ISO): Geneva, Switzerland, 2007.
32. Collivignarelli, M.C.; Abbà, A.; Carnevale Miino, M.; Arab, H.; Bestetti, M.; Franz, S. Decolorization and Biodegradability of a Real Pharmaceutical Wastewater Treated by H<sub>2</sub>O<sub>2</sub>-Assisted Photoelectrocatalysis on TiO<sub>2</sub> Meshes. *J. Hazard. Mater.* **2020**, *387*, 121668. <https://doi.org/10.1016/j.jhazmat.2019.121668>.
33. Tauchert, E.; Schneider, S.; de Morais, J.L.; Peralta-Zamora, P. Photochemically-Assisted Electrochemical Degradation of Landfill Leachate. *Chemosphere* **2006**, *64*, 1458–1463. <https://doi.org/10.1016/j.chemosphere.2005.12.064>.

34. Collivignarelli, M.C.; Abbà, A.; Caccamo, F.M.; Carnevale Miino, M.; Durante, A.; Bellazzi, S.; Baldi, M.; Bertanza, G. How to Produce an Alternative Carbon Source for Denitrification by Treating and Drastically Reducing Biological Sewage Sludge. *Membranes* **2021**, *11*, 977. <https://doi.org/10.3390/membranes11120977>.
35. Collivignarelli, M.C.; Carnevale Miino, M.; Caccamo, F.M.; Baldi, M.; Abbà, A. Performance of Full-Scale Thermophilic Membrane Bioreactor and Assessment of the Effect of the Aqueous Residue on Mesophilic Biological Activity. *Water* **2021**, *13*, 1754. <https://doi.org/10.3390/w13131754>.
36. ISPRA *Measurement Procedure for the Determination of the Chemical Oxygen Demand (COD) by Cuvette Test: Method 5135 (in Italian)*; Higher Institute for Environmental Protection and Research: Rome, Italy, 2014.
37. Franz, S.; Falletta, E.; Arab, H.; Murgolo, S.; Bestetti, M.; Mascolo, G. Degradation of Carbamazepine by Photo(Electro)Catalysis on Nanostructured TiO<sub>2</sub> Meshes: Transformation Products and Reaction Pathways. *Catalysts* **2020**, *10*, 169. <https://doi.org/10.3390/catal10020169>.
38. Garcia-Segura, S.; Brillas, E. Applied Photoelectrocatalysis on the Degradation of Organic Pollutants in Wastewaters. *J. Photochem. Photobiol. C Photochem. Rev.* **2017**, *31*, 1–35. <https://doi.org/10.1016/j.jphotochemrev.2017.01.005>.
39. Zertal, A.; Molnár-Gábor, D.; Malouki, M.A.; Sehili, T.; Boule, P. Photocatalytic Transformation of 4-Chloro-2-Methylphenoxyacetic Acid (MCPA) on Several Kinds of TiO<sub>2</sub>. *Appl. Catal. B* **2004**, *49*, 83–89. <https://doi.org/10.1016/J.APCATB.2003.11.015>.
40. Chow, H.; Ingelsson, M.; Roberts, E.P.L.; Pham, A.L.-T. How Does Periodic Polarity Reversal Affect the Faradaic Efficiency and Electrode Fouling during Iron Electrocoagulation? *Water Res.* **2021**, *203*, 117497. <https://doi.org/10.1016/j.watres.2021.117497>.
41. Bandaru, S.R.S.; Roy, A.; Gadgil, A.J.; van Genuchten, C.M. Long-Term Electrode Behavior during Treatment of Arsenic Contaminated Groundwater by a Pilot-Scale Iron Electrocoagulation System. *Water Res.* **2020**, *175*, 115668. <https://doi.org/10.1016/j.watres.2020.115668>.

**Disclaimer/Publisher's Note:** The statements, opinions and data contained in all publications are solely those of the individual author(s) and contributor(s) and not of MDPI and/or the editor(s). MDPI and/or the editor(s) disclaim responsibility for any injury to people or property resulting from any ideas, methods, instructions or products referred to in the content.